AIP | Applied Physics Letters

Mott-type MgxZn1-xO-based visible-blind ultraviolet photodetectors with active anti-reflection layer

X. H. Xie, Z. Z. Zhang, B. H. Li, S. P. Wang, M. M. Jiang, C. X. Shan, D. X. Zhao, H. Y. Chen, and D. Z. Shen

Citation: Applied Physics Letters **102**, 231122 (2013); doi: 10.1063/1.4811153
View online: http://dx.doi.org/10.1063/1.4811153
View Table of Contents: http://scitation.aip.org/content/aip/journal/apl/102/23?ver=pdfcov
Published by the AIP Publishing

Mott-type $Mg_xZn_{1-x}O$-based visible-blind ultraviolet photodetectors with active anti-reflection layer

X. H. Xie,[1,2] Z. Z. Zhang,[1,a)] B. H. Li,[1] S. P. Wang,[1] M. M. Jiang,[1] C. X. Shan,[1] D. X. Zhao,[1] H. Y. Chen,[1,2] and D. Z. Shen[1,b)]
[1]*State Key Laboratory of Luminescence and Applications, Changchun Institute of Optics, Fine Mechanics and Physics, Chinese Academy of Sciences, Changchun 130033, People's Republic of China*
[2]*University of Chinese Academy of Sciences, Beijing 100049, People's Republic of China*

(Received 17 March 2013; accepted 30 May 2013; published online 12 June 2013)

We report on a vertical geometry Mott-type visible (VIS)-blind Ultraviolet (UV) photodetector which was fabricated based on wurzite MgZnO (W-MgZnO) with a cubic MgZnO (C-MgZnO) anti-reflection layer. The C-MgZnO layer plays two roles in the detector, not only the conventional optical part but also electrical part. Photon-generated holes were restricted due to valence band offset. More "hot" electrons injected over a reduced Mott potential barrier at the metal-semiconductor interface, resulting in additional current contributing to photoresponse. This dual-function structure is a highly compact and wavelength-resonant UV detector, with a spectral response high-gain and fast. © *2013 AIP Publishing LLC*. [http://dx.doi.org/10.1063/1.4811153]

Ultraviolet (UV) photodetectors based on wide bandgap semiconductors have attracted much attention in recent years for their potential applications, including flame sensing, UV-photography, chemical/biological agent detection, free space communications, missile plume sensing, and UV-astronomy, etc.[1–5] MgZnO with tunable band gaps is a very promising candidate for fabricating visible (VIS)- and solar-blind ultraviolet photodetectors. Depending on the magnesium mole fraction in the MgZnO layer, the cutoff wavelength of the device can be tuned between 225 and 370 nm to fit the requirements of the specific application.[6–9] By far, different MgZnO-based UV detectors structures have been presented, including metal-semiconductor-metal (MSM),[10] single Schottky,[11] and p-n heterojunction diodes.[12] An important advancement in the field of VIS-blind MgZnO-based photodetectors has been the development of devices capable of photoconductive gain.[13–16] In these detectors, electron-hole pair generation is followed by the trapping of one of the charge carriers. If the trap lifetime (t_{life}) exceeds the transit time ($t_{extract}$) of the opposite charge carrier, majority carriers, worth of current, can pass through the circuit many times until recombination occurs. Although these high photoconductive gains increase responsivity, they also reduce the devices' bandwidth due to the long circulating carrier lifetimes involved. Especially, the presence of persistent photocurrent (PPC) of the planar devices, owing to the surface adsorption,[16] can extremely reduce the recover time of the detectors, which is typically in the order of seconds. Another factor, influencing the response speed of the photodetectors, is the junction capacitance, which can be ascribed to the carrier concentration of the semiconductor.

A Mott barrier,[17] as defined, is a metal-semiconductor contact in that the surface layer is lightly doped so that the whole epitaxial layer is fully depleted. Usually, it has better frequency performance compared with the Schottky barrier on account of its lower series resistance-junction capacitance product.

Meanwhile, in past decade, design of active cladding with "smart" behavior such as active optical antennas,[18] plasmon-sensitized solar cell,[19] etc., have produced elements that can facilitate the figure of merit of device. The refractive index and band-gap can be adjusted by changing the magnesium mole fraction in the MgZnO films. It is attractive that to integrate conventional anti-reflection layer with a function of control the carriers transport.

We fabricate, in this work, a Mott-type vertical geometry VIS-blind UV photodetector with a lightly Ga-doped cubic MgZnO (C-MgZnO) surface epitaxial layer (as the anti-reflection layer at one time), which has not been reported elsewhere. C-MgZnO, due to its larger bandgap and higher conduction band minimum than wurzite MgZnO (W-MgZnO), possesses much deeper donor levels, which will result in lower carrier concentration,[20] and then the smaller parasitic capacitance. The device exhibits relative high gain without PPC effect, which is both fast and efficient. The study of the double-layer crystal structure and optoelectronic properties for the devices was carried out, via the transmission spectrum, x-ray diffraction (XRD), current-voltage (*I-V*), spectral response, and temporal response measurements. Especially, the temporal response, in high gain detectors, was rarely investigated yet.[14,15]

The device vertical structure was grown on c-plane sapphire substrate by metal-organic chemical vapor deposition (MOCVD). Diethylzinc (DEZn), Dimethyl dicyclopentadienyl magnesium ($MeCp_2Mg$), and high pure oxygen (O_2) were employed as the precursors. Triethylgallium (TEGa) was used as the dopant source. High purity nitrogen (99.999%) acts as a carrier for the metal-organic (MO) sources. The MOCVD chamber pressure was kept at 200 Torr and the substrate temperature at 450 °C during the growth process. About 600 nm-thick Ga doped W-MgZnO was first deposited on top of about 50 nm-thick W-MgZnO buffer layer. Subsequently, a lightly Ga-doped C-MgZnO, about 400 nm, was deposited. The flux ratio for [TEGa]/([DEZn]+[$MeCp_2Mg$]) was fixed in 1:500

a)Author to whom correspondence should be addressed. Electronic mail: exciton@163.com
b)dzshen824@sohu.com

and 1:1800, respectively, for the W-MgZnO and C-MgZnO growth. More growth details about W- and C-MgZnO can be found elsewhere.[21,22] A schematic diagram of the device is illustrated in Fig. 1.

The transmission spectra of W-MgZnO and C-MgZnO, which were deposited during each experiment, were recorded by employing a Shimadzu UV-3101PC scanning spectrophotometer. The structural characterization of the double-layers thin film was evaluated by XRD with Cu-Kα 0.154 nm line as the radiation source. Au and Indium metal electrodes were fabricated on the C-MgZnO and W-MgZnO, respectively, using vacuum evaporation and masking methods. Hall measurement system (Lake Shore HMS7707) was employed for *I-V* characterization. The spectral response of the detector was measured using a 150 W Xe arc lamp, a monochromator, an optical chopper (EG&G 192), and a lock-in amplifier (EG&G 124A) in a synchronous detection scheme. The temporal response was performed using the same system of spectral response measurement, in addition, with a Keithley 2611A System SourceMeter to record the photocurrent-time relation of the detector.

Figure 2(a) shows the typical transmission spectra of ZnO, W-MgZnO, and C-MgZnO. By the way, each film was deposited in the same experiment which grown W-MgZnO and C-MgZnO, respectively. All the films show sharp transmission edge and high transmittance of about 90% in the visible region, which indicates the good optical quality of the samples. As shown in the spectra, the absorption edge of the W- and C-MgZnO films located at around 365 nm and 260 nm, respectively, corresponds to the optical band gap of 3.40 eV and 4.70 eV. It is noteworthy that the UV interference extremum of C-MgZnO are located around the peaks of detector responsivity, seen below, which can be indicated the film plays the anti-reflection effect for this device. The structural characterizations of the vertical structure were assessed by XRD, as shown in Fig. 2(b). Two obvious peaks located at 34.56° and 36.62° can be observed in the θ-2θ XRD pattern, which are attributed to the (002) diffraction of W-MgZnO and (111) diffraction of C-MgZnO, respectively. Typical XRD patterns of W- and C-MgZnO films were shown in the inset of Fig. 2(b). The above results confirmed that the vertical structure was combined with W-MgZnO and C-MgZnO. (Indium bonding pads, which were used to protect the electrodes, account for the weak diffraction peaks (32.95°, 39.18°).)

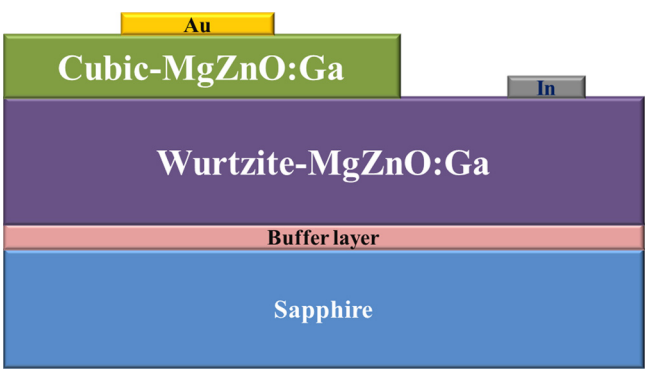

FIG. 1. Schematic diagram of the C-MgZnO/W-MgZnO based VIS-blind UV photodetector in side view.

The *I-V* curve of the vertical geometry Mott-type photodetector is shown in Fig. 3(a). The asymmetrical rectifying behavior indicates that a barrier exists between Au and In electrode. Additionally, as can be seen in Fig. 3(b), the *I-V* curve of In/W-MgZnO/In shows a straight line, illustrating a good ohmic contact. So it can be deduced that a Mott-type barrier was formed in the device structure. No sharp breakdown or saturation of current was observed in the measurement range from −60 V to 60 V. It suggests that the detector could work in high-power circuits.

Figure 4(a) shows the spectral response of the detector at 15 V and 30 V bias. It shows a VIS-blind UV detection capability with a cutoff at 362 nm. The peak responsivity of about 431 mA/W at 30 V bias is located at 325 nm, corresponding to an external quantum efficiency (EQE) of 165%. As a fundamental parameter for evaluating the photodetector performance, $R_\lambda = I_{ph}/P_{opt} = \eta q/h\nu$,[17] ($\eta = 1,\ 0.6,\ 0.4$), is plotted as a function of incident light wavelength, where h is Plank's constant, ν is the frequency of incident light, and η is the quantum efficiency. There are four peaks in the spectrum, located UV-A/-B/-C respectively, which correspond to the band-edge photoresponse of W-MgZnO, C-MgZnO, and the wavelength-resonant of anti-reflection layer (see Figure 2(a)). As shown in Fig. 4(b), the maximum responsivity at 325 nm increases monotonically with the applied bias. When the bias is greater than 23 V, the responsivity exceeds

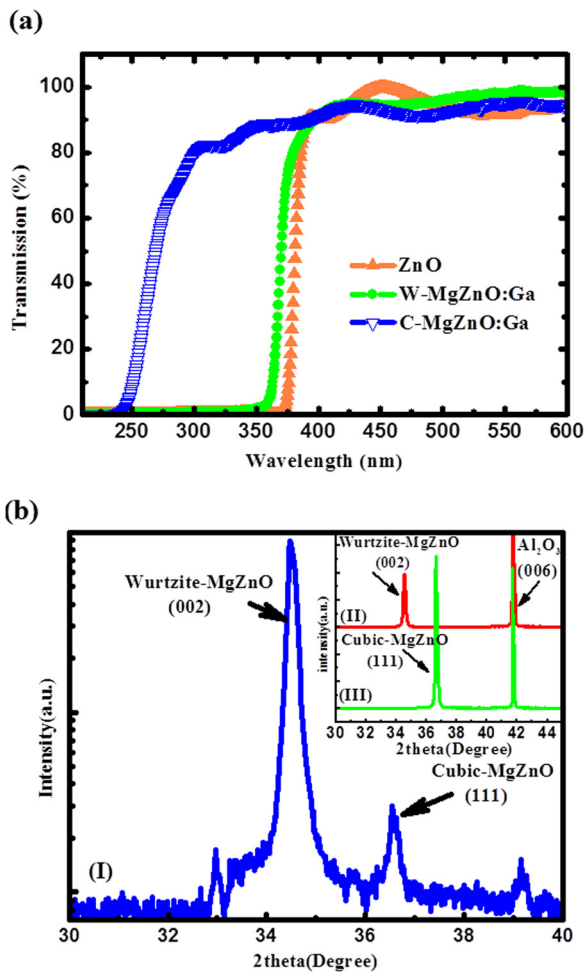

FIG. 2. (a) Transmission spectrum of the ZnO, wurtzite MgZnO, and cubic MgZnO films. (b) θ-2θ XRD spectrum of the vertical structure.

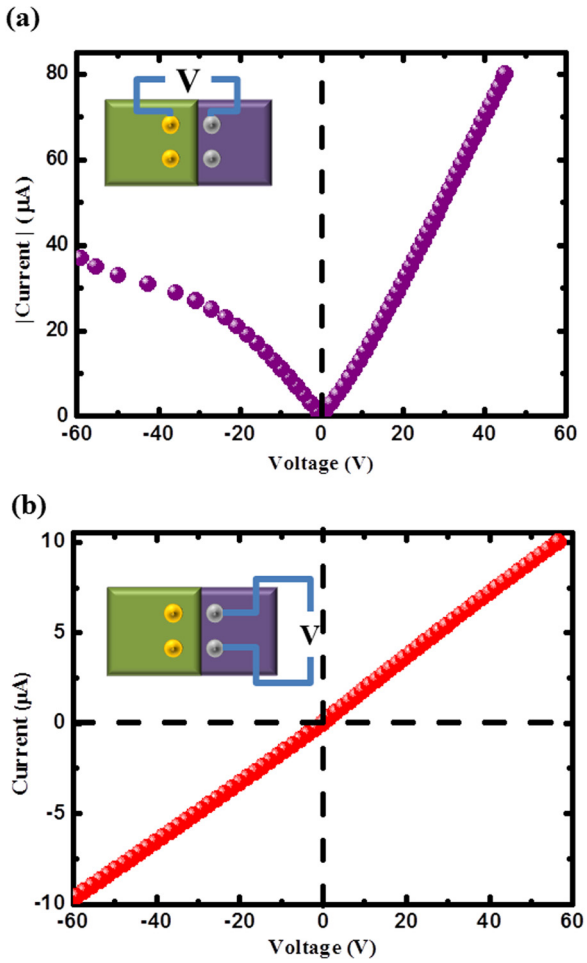

FIG. 3. (a) I–V characteristic of the Mott-type UV photodetector. (b) I–V characteristic of the In/W-MgZnO/In.

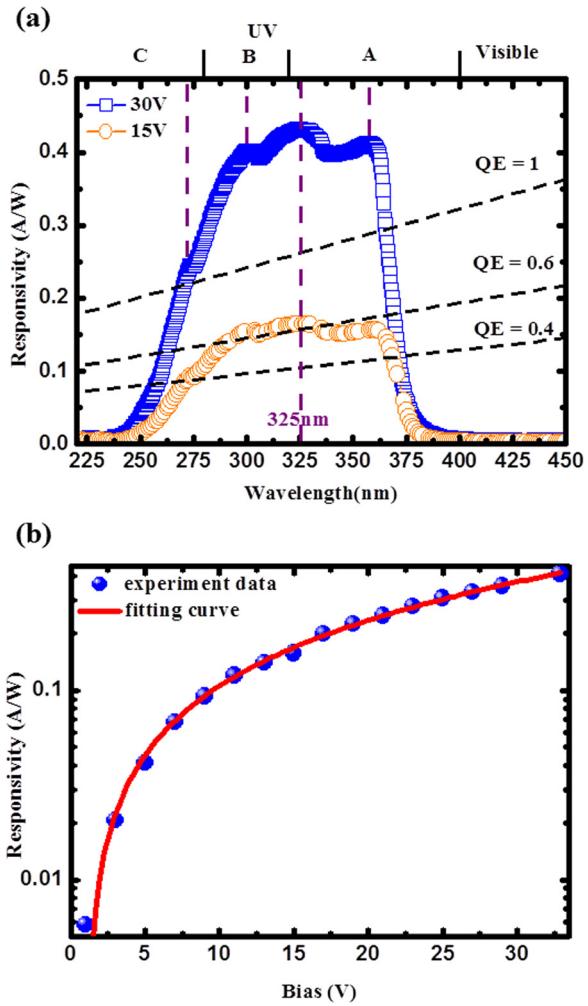

FIG. 4. (a) Spectral response of the Mott-type photodetector at bias 15 V and 30 V. (b) The dependence of the maximum responsivity of the photodetector on the bias applied.

277.4 mA/W, corresponding to an EQE beyond 100%. It indicates a large internal gain. Further, the experiment data in high bias range, follow a linear relation, which indicate that such gain cannot be generated by the photoconductive gain mechanism.[23] A reduced Mott-barrier height model,[17,24,25] $R_\lambda = \{[\exp(\Delta\varphi_b/kT) - 1]I_{\text{dark}} - I_\lambda\}/W$, (where kT is the thermal energy, $\Delta\varphi_b$ is reduced barrier height, W is the light intensity, I_{dark} and I_λ is darkcurrent and photocurrent, respectively), is adopted to explain the gain mechanism in this work. Using this model, the fitting curve agrees well with the experimental data.

In order to better visualize the gain mechanism of the detector, the energy band diagrams derived from Anderson model are shown in Fig. 5 for further discussion. Fig. 5(a) shows the band alignment of the Mott-type photodetector at zero bias. Under the light irradiation at reverse bias, as shown in the Fig. 5(b), there are two parts contributing to the photoresponse. The "I-current" is caused by the carriers optically generated in the depletion region. The "II-current" is due to the lowering of the Mott barrier, which is caused by restricting of the photogenerated holes at interface between W-MgZnO and C-MgZnO. The contribution of "II mechanism" makes the EQE exceed 100%, or generate the gain.

The temporal response of the VIS-blind photodetector was shown in Fig. 6. The photocurrent of the detector was measured at different bias (0.5 V to 10 V) when the irradiation light (325 nm) was chopped at 90 Hz, as shown in Fig. 6(a). It can be seen that when the UV illumination is on/off, photocurrent of the device quickly reaches/returns to its maximum/initial value. It indicates that the device has a fast response to the

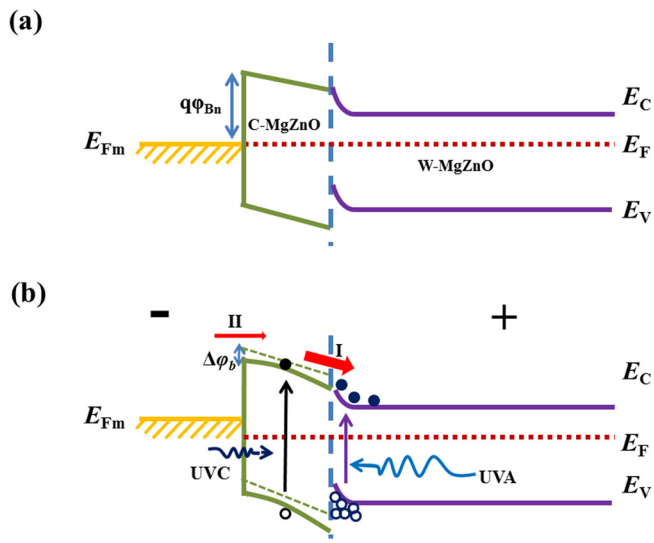

FIG. 5. Schematic diagram showing the band alignment of the Mott-type photodetector (a) under equilibrium condition and (b) under illumination at reverse bias.

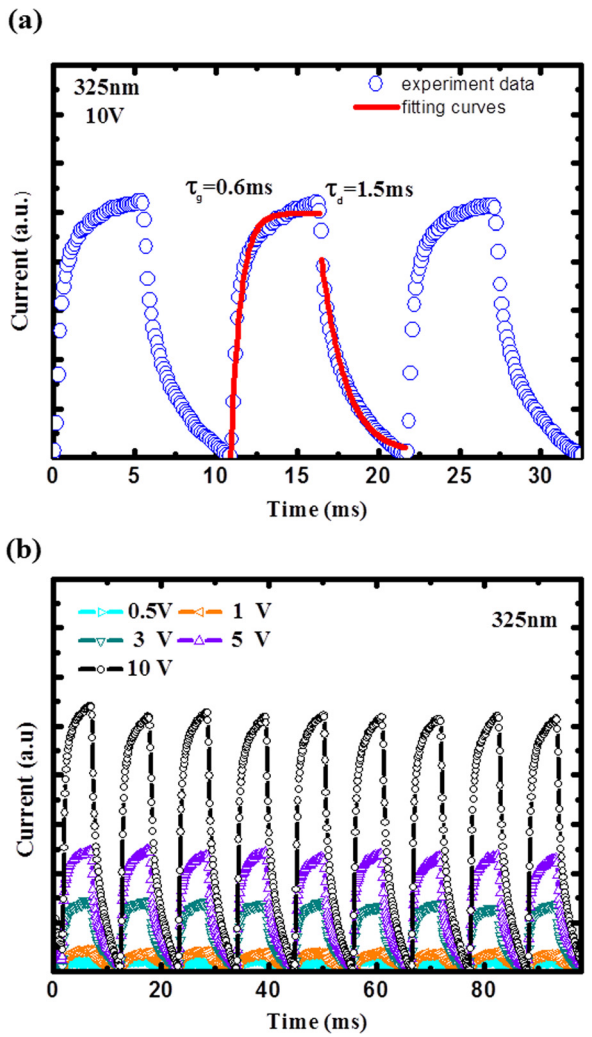

FIG. 6. (a) Time-dependent response of the photocurrent of device. (b) Photocurrent transient at a bias voltage of 10 V.

light irradiation. Figure 6(b) shows the photocurrent transient for illumination, which indicates a good stability for UV photoresponse. Upon irradiation, the photoresponse follows a first-order exponential growth function with an estimated time constant of $\tau_g = 0.6$ ms. When the UV light is chopped, the photoresponse follows the first-order exponential, too ($\tau_d = 1.5$ ms). Such a decay trend indicates that there exists no PPC effect.[26,27] Also, due to the large longitudinal electric field in the vertical geometry device, the photo-generated carriers are separated immediately and drifted to the electrodes.

In conclusion, we investigated a Mott-type VIS-blind UV photodetector with active anti-reflection layer based on a C-MgZnO/W-MgZnO vertical structure for high gain and fast photoresponse. The maximum responsivity is 431 mA/W under 30 V. The detector shows a fast response for UV irradiation with $\tau_g = 0.6$ ms and $\tau_d = 1.5$ ms. Such kind of device may be a choice to realize the UV photon detection, based on MgZnO or even other wide bandgap material, combined the fast response times with high efficiencies. By optimizing the device structure more accurately, such as multiple-layers structure, it is probable to obtain a larger gain bandwidth product of the MgZnO-based UV photodetector.

This work is supported by the National Basic Research Program of China (973 Program) under Nos. 2011CB302002 and 2011CB302006, the National Natural Science Foundation of China under Nos. 11134009 and 11104265.

[1]G. Konstantatos and E. H. Sargent, Nat. Nanotechnol. **5**(6), 391–400 (2010).
[2]C. J. Collins, U. Chowdhury, M. M. Wong, B. Yang, A. L. Beck, R. D. Dupuis, and J. C. Campbell, Appl. Phys. Lett. **80**(20), 3754–3756 (2002).
[3]Y. Q. Bie, Z. M. Liao, H. Z. Zhang, G. R. Li, Y. Ye, Y. B. Zhou, J. Xu, Z. X. Qin, L. Dai, and D. P. Yu, Adv. Mater. **23**(5), 649–653 (2011).
[4]T. Tut, M. Gokkavas, A. Inal, and E. Ozbay, Appl. Phys. Lett. **90**(16), 163506 (2007).
[5]L. K. Wang, Z. G. Ju, J. Y. Zhang, J. Zheng, D. Z. Shen, B. Yao, D. X. Zhao, Z. Z. Zhang, B. H. Li, and C. X. Shan, Appl. Phys. Lett. **95**(13), 131113 (2009).
[6]S. Han, Z. Z. Zhang, J. Y. Zhang, L. K. Wang, J. Zheng, H. F. Zhao, Y. C. Zhang, M. M. Jiang, S. P. Wang, D. X. Zhao, C. X. Shan, B. H. Li, and D. Z. Shen, Appl. Phys. Lett. **99**(24), 242105 (2011).
[7]Z. P. Zhang, H. von Wenckstern, M. Schmidt, and M. Grundmann, Appl. Phys. Lett. **99**(8), 083502 (2011).
[8]Z. G. Ju, C. X. Shan, D. Y. Jiang, J. Y. Zhang, B. Yao, D. X. Zhao, D. Z. Shen, and X. W. Fan, Appl. Phys. Lett. **93**(17), 173505 (2008).
[9]Y. M. Zhao, J. Y. Zhang, D. Y. Jiang, C. X. Shan, Z. Z. Zhang, B. Yao, D. X. Zhao, and D. Z. Shen, ACS Appl. Mater. Inter. **1**(11), 2428–2430 (2009).
[10]L. K. Wang, Z. G. Ju, C. X. Shan, J. Zheng, D. Z. Shen, B. Yao, D. X. Zhao, Z. Z. Zhang, B. H. Li, and J. Y. Zhang, Solid State Commun. **149**(45–46), 2021–2023 (2009).
[11]S. Han, J. Y. Zhang, Z. Z. Zhang, L. K. Wang, Y. M. Zhao, J. Zheng, J. M. Cao, B. Yao, D. X. Zhao, and D. Z. Shen, J. Phys. Chem. C **114**(49), 21757–21761 (2010).
[12]H. L. Liang, Z. X. Mei, Q. H. Zhang, L. Gu, S. Liang, Y. N. Hou, D. Q. Ye, C. Z. Gu, R. C. Yu, and X. L. Du, Appl. Phys. Lett. **98**(22), 221902 (2011).
[13]C. Soci, A. Zhang, B. Xiang, S. A. Dayeh, D. P. R. Aplin, J. Park, X. Y. Bao, Y. H. Lo, and D. Wang, Nano Lett. **7**(4), 1003–1009 (2007).
[14]G. Tabares, A. Hierro, J. M. Ulloa, A. Guzman, E. Munoz, A. Nakamura, T. Hayashi, and J. Temmyo, Appl. Phys. Lett. **96**(10), 101112 (2010).
[15]A. Hierro, G. Tabares, J. M. Ulloa, E. Munoz, A. Nakamura, T. Hayashi, and J. Temmyo, Appl. Phys. Lett. **94**(23), 232101 (2009).
[16]Y. Z. Jin, J. P. Wang, B. Q. Sun, J. C. Blakesley, and N. C. Greenham, Nano Lett. **8**(6), 1649–1653 (2008).
[17]S. M. Sze and K. K. Ng, *Physics of Semiconductor Devices*, 3rd ed. (Wiley, Hoboken, 2007).
[18]M. W. Knight, H. Sobhani, P. Nordlander, and N. J. Halas, Science **332**(6030), 702–704 (2011).
[19]Y. H. Su, Y. F. Ke, S. L. Cai, and Q. Y. Yao, Light: Sci. Appl. **1**, e14 (2012).
[20]Y. F. Li, B. Yao, Y. M. Lu, Z. P. Wei, Y. Q. Gai, C. J. Zheng, Z. Z. Zhang, B. H. Li, D. Z. Shen, X. W. Fan, and Z. K. Tang, Appl. Phys. Lett. **91**(23), 232115 (2007).
[21]X. H. Xie, Z. Z. Zhang, C. X. Shan, H. Y. Chen, and D. Z. Shen, Appl. Phys. Lett. **101**(8), 081104 (2012).
[22]L. K. Wang, Z. G. Ju, C. X. Shan, J. Zheng, B. H. Li, Z. Z. Zhang, B. Yao, D. X. Zhao, D. Z. Shen, and J. Y. Zhang, J. Cryst. Growth **312**(7), 875–877 (2010).
[23]J. A. Garrido, E. Monroy, I. Izpura, and E. Muñoz, Semicond. Sci. Technol. **13**, 563–568 (1998).
[24]O. Katz, V. Barber, B. Meyler, G. Bahir, and J. Salzman, Appl. Phys. Lett. **79**, 1417 (2001).
[25]A. Sciuto, F. Roccaforte, S. Di Franco, V. Raineri, S. Billotta, and G. Bonanno, Appl. Phys. Lett. **90**, 223507 (2007).
[26]J. B. K. Law and J. T. L. Thong, Appl. Phys. Lett. **88**(13), 133114 (2006).
[27]M. Martens, J. Schlegel, P. Vogt, F. Brunner, R. Lossy, J. Wurfl, M. Weyers, and M. Kneissl, Appl. Phys. Lett. **98**(21), 211114 (2011).